



Enhanced Topical Delivery Of Azelaic Acid Through Nanoemulsion Formulation: Optimization, Characterization, And Potential Therapeutic Application For Skin Disorders

Rahisuddin^{1*}, Nasiruddin Ahmad Farooqui², Dinesh Kumar Sharma³,

¹Research Scholar, Sanskriti University, Mathura-Delhi Highway, Chhata, Mathura, 281401, U.P., India

²Professor, Translam Institute of Pharmaceutical Education and Research, Meerut, 250001, U.P., India

³Professor, Sanskriti University, Mathura-Delhi Highway, Chhata, Mathura, 281401, U.P., India

*Corresponding Author: Rahisuddin

Email ID- raiseder@yahoo.in

Abstract

Rapid connectivity homogenization and ultra-probe sonication were used to manufacture the Azelic acid nanoemulsion. Everything is dissolved in clean water: Azelic acid, polyvinyl alcohol, xanthan gum, castor oil, vitamin E, Transcutol P, and Tween 80. To optimize it, we used Response Surface Methodology and measured a bunch of parameters, like droplet size (nm), surface morphology (FE-SEM, TEM), zeta potential (ZP), differential scanning calorimetry (DSC), polydispersity index (PDI), stability, pH, and viscosity. Both the penetration and retention of the Azelic acid -loaded nanoemulsion into the skin and its release profile were studied in vitro and ex vivo, respectively. The model's quadratic polynomial fitness was confirmed by the optimization analysis of variance (ANOVA), which yielded a significant F-value and a p-value below 0.0500. It was also determined that the lack-of-fit was not statistically significant. Globule size was 200 nm, PDI was 0.2, and entrapment efficacy was 84.99% following optimization of the Azelic acid nanoemulsion. A value of -35.90 mV was recorded for the Zeta Potential (ZP). The absence of chemical interactions was verified by the findings of FTIR, DSC, and XRD investigations, which demonstrated the effective trapping of Azelic acid. Results from scanning electron microscopy and transmission electron microscopy revealed the presence of small spherical particles in the enhanced formulation. Centrifugation, freeze-thaw cycles, and storage at 5°C and 25°C were all successfully completed by the sample in the stability tests. Storage at 40°C for 7 weeks resulted in subtle color shifts, most noticeably during the last week of the study. The results of the rheological tests showed that the revised recipe is elastic and May shear-thin and pseudo-plastic. Over the course of 12 hours, the Azelic acid nanoemulsion released 87.66 % and 97.99 of its active ingredient. A high degree of linearity was demonstrated by the sustained release pattern, which matched a zero-order kinetic model ($R^2 = 0.9952$). After 8 hours, the Azelic acid nanoemulsion had an ex vivo penetration rate of 82.24 %, indicating better skin distribution. Based on the results, Azelic acid nanoemulsion might be useful as a skin condition topical therapy. Nevertheless, further research, including studies conducted in living organisms, is necessary to prove that azelic acid nanoemulsion is both efficient and safe.

CC License
CC-BY-NC-SA 4.0

1. Introduction:

Skin hyperpigmentation disorders, characterized by the abnormal accumulation of melanin, pose a significant challenge in dermatology, impacting the physical and psychological well-being of affected individuals. Conditions such as melasma, post-inflammatory hyperpigmentation, and age-related spots often result in uneven skin tone, reduced self-esteem, and an increased demand for effective therapeutic interventions. Azelaic acid, a naturally occurring dicarboxylic acid with well-established anti-inflammatory and depigmenting properties, has emerged as a promising candidate for addressing hyperpigmentation disorders. While azelaic acid has demonstrated efficacy in various dermatological applications, its penetration into the skin remains a limiting factor, hindering its optimal therapeutic potential. Nanoemulsions, colloidal dispersions with droplet sizes typically ranging from 20 to 200 nanometers, present a novel and efficient platform for enhancing the delivery of lipophilic compounds like azelaic acid. The unique physicochemical properties of nanoemulsions, including increased surface area and improved stability, make them ideal carriers for enhancing drug permeation through the skin barrier[1].

2. Material and Methods:

2.1 Preparation of azelic acid loaded Nano emulsion

Aqueous phase

0.5 % PVA was dispersed in distilled water and heated at 70 °C to dissolve it. 0.7 % xanthan gum was also swelled in another beaker then 100mg azelic acid added. After complete mixing PVA solution was added to it and mixed using magnetic stirrer at 700-800 rpm to make aqueous phase. In another beaker 3 % tween 80 & 1 % transcutool P were mixed [2].

Oil phase

3.50 % castor oil, & 1 % Vitamin E were mixed and stirred using magnetic stirrer at 700-800 rpm to form a homogenous solution.

Oil phase was added dropwise into aqueous phase while heated at 30 °C and stirred at 700- 800 rpm for 1hr using magnetic stirrer.

Then, the mixture was further homogenized for 15 min at 8000 rpm using a homogenizer. While mixture was homogenized tween 80 & transcutool P mixture was added to it. Finally, mixture was sonicated using probe sonicator for 5 min to get proper nano size.

2.2 Selection of the Nanoemulsion Components

2.2.1 Solubility studies in oil

The solubility of azelic acid was investigated in various oils (peppermint oil, vitamin E, and castor oil). In order to find solubility of Azelic acid, the excess amount of drug was added in each 2 ml of oil, in 5ml capacity stoppered vials and mixed for 10 minutes by vortex mixer. The vials were placed in bath shaker at 25 ± 0.5 °C for 48 hrs to reach equilibrium. The samples were removed after achieving equilibrium and centrifuged at 4000 RPM for 15 minutes using centrifuge and the collected supernatant was filtered through a 0.45 μ m membrane filter. After filtration, samples were further diluted with ethanol. The concentration of azelic acid in each sample was determined using UV-Visible spectrophotometer at λ max 269 nm using a standard calibration curve of azelic acid [3].

2.2.2 Screening of components for nanoemulsion

Oil was selected based on the maximum solubilization amount of azelic acid in different oil. The percent transmittance of emulsification is criteria for the selection of surfactant and co-surfactant for nano-emulsion formulation. The emulsification potential of surfactant and cosurfactant (Tween 80, poloxamer 188, poloxamer 407 and transcutool P) was determined by adding 2 ml surfactant/ cosurfactant in 2 ml selected oil phase. The mixture was then subjected to heat at 40 °C to 45 °C to attain homogenization. From the resulted mixture were filtered, then 1 ml taken and diluted with double distilled water to produce fine emulsion. Then emulsion was allowed to stand for 2 hrs, inspected visually for any relative turbidity and % transparency was evaluated by UV-VIS spectroscopy at 269 nm using distilled water as blank[4].

2.2.3 Experimental design

In the design of Azelic acid nanoemulsion, different factors play a critical role in developing an optimized batch. Response surface methodology (RSM) is the most applied statistical model for optimization of Azelic

acid nanoemulsion [5]. For this study, three levels-three factor design was required and hence among the various techniques of response surface methodology (RSM), Box–Behnken statistical design (BBD) with three factors was selected. Because Box-Behnken designs statistically optimized the formulation parameters with a relatively small number of experimental runs, and they can be less expensive to do than central composite designs with the same number of factors [195,196]. Box–Behnken design has been successfully used to optimize the technology or production conditions for drug delivery systems such as nanoemulsion, micro emulsion, liposomes, and microsphere in recent years.

2.2.4 Formulation optimization using Box-Behnken experimental design

A three-factor, three-level Box-Behnken Design was developed by software of experimental design (Design Expert® Version 11, Stat-ease Inc., Minneapolis) which resulted in 17 experimental runs. BBD is a three-factor, three-level statistical screening approach which was applied in our study to evaluate main, interaction and quadratic effects of the formulation variables [(PVA: Xanthan gum), (Tween 80: Transcutol P), and Homogenization speed] on measured responses [particle size, polydispersity index (PDI) and entrapment efficiency] of prepared Azelic acid nanoemulsion and applicability of desirability function to optimize the formulation. 3-factorial design was used to explore the quadratic response surfaces and for constructing contour plot and second order polynomial models. The non-linear quadratic model equation produced by the BBD is of the form (Eq. 1):

$$Y = \alpha_0 + \alpha_1A + \alpha_2B + \alpha_3C + \alpha_4AB + \alpha_5BC + \alpha_6AC + \alpha_7A^2 + \alpha_8B^2 + \alpha_9C^2 \dots(1)$$

where, Y is the dependent or measured response of the dependent variables associated with each factor-level combination; α_0 is the intercept; α_1 – α_9 are the regression coefficients; while PVA: Xanthan gum (A), Tween 80: Transcutol P (B),and Homogenization speed (C) were selected as the independent variables and particle size (Y1), polydispersity index (Y2) and % drug entrapment efficiency (Y3) were selected as the responses because they are generally considered as significant factors for assessing the qualities of nanoemulsion [6]. The independent and dependent variables selected are shown in Table 6.1 along with their high, medium and low levels. Optimized formulation was selected on the basis of minimum particle size, minimum PDI value and maximum Entrapment Efficiency of the formulation.

Table 1: Independent and dependent variables range lower to higher

Factors	Coded Levels		
	Low (-1)	Medium (0)	high (+1)
X1= PVA: Xanthan gum (%)	0.6	1.4	1.6
X2= Tween 80: Transcutol P (%) [3:1]	1.30	2	6
X3=Homogenization speed (RPM)	3100	6400	10000
Dependent variables	Constraints		
Y1=Size (nm)	Minimum (100)		
Y2= Polydispersity Index (PDI)	Minimum		
Y3= Entrapment Efficiency	Maximum (100%)		

Table 2: Experimental sample for Box-Behnken design

Std	Sample	Factor 1 A: PVA: Xanthan %	Factor 2 B: Tween 80: Tra %	Factor 3 C: Homoge nization RPM	Response 1 Particle size	Response 2 PDI	Response 3 %EE
11	1	1.3	1	10000	202	0.2	75
16	2	1.3	2	6400	185	0.3	85.84
5	3	0.8	2	3100	172	0.2	70
4	4	1.5	5	6400	277	0.5	51
7	5	0.8	3	10000	198	0.4	82
14	6	1.1	3	6400	185	0.3	85.84
6	7	1.5	3	3100	275	0.7	83
10	8	1.1	2	3100	210	0.4	82
3	9	0.8	5	6400	206	0.2	65
1	10	0.8	5	6400	206	0.4	58
8	11	1.5	2	10000	190	0.2	64
2	12	1.1	1	6400	244	0.4	64

17	13	1.1	2	6400	264	0.3	85.84
12	14	1.1	5	10000	185	0.3	68
15	15	1.1	2	6400	186	0.5	85.84
13	16	1.1	2	6400	185	0.3	85.84
9	17	1.1	1	3100	185	0.5	79

2.2.5 Statistical analysis

All data were obtained using Design Expert 11. Each response was separately fitted to a full quadratic equation; significance of model was assessed by ANOVA, and multiple correlation coefficient (R²) tests. The design consists of replicated centre points and the set of points lying at the midpoint of each edge of the multidimensional cube that defines the region of interest. For the model to be fitted well in the quadratic equation, the model p value should be less than 0.05 (significant). The amount of variation around the mean is expressed by R² value (multiple correlation coefficient tests). The value of R² should be close to 1 [7,8]. The response surface analysis plots in three-dimensional model graphs were constructed using the software. These plots were used to study the interaction effects of two independent variables on the responses while holding the third factor at a constant level.

2.2.6 Fourier Transform Infrared (FTIR) Analysis

FTIR analysis was done to certify the encapsulation of azelic acid in the NLC and for the detection of intermolecular interactions between the API and the excipients through the vibrational changes [9]. A reduction of the peak intensity, the appearance of an absorption peak, or the appearance of new peaks indicate the existence of interactions between the excipient and the API [10]. The sample of azelic acid nanoemulsion was evaluated using FT-IR spectrophotometer with a wavelength of 400 cm⁻¹ to 4000 cm⁻¹. In FTIR spectra analysis, a small amount of liquid sample was used and a thin film was allowed to form on a KBr pellet and spectra were recorded.

2.2.7 Thermal Analysis

Thermo-analytical techniques have been developed to predict the suitability of the excipients to be employed in dosage forms in order to minimize undesired reactions (stability issues) between the API and the excipient [11]. The thermal analyses of xanthan gum, titanium dioxide-based polyurethanes were performed by Thermo gravimetric analysis (TGA) and Differential Scanning Calorimetric (DSC). These analyses are further explained below.

2.2.7.1 Differential Scanning Calorimetric (DSC)

DSC technique was examined to analyze the matrix structure and thermal behaviour of azelic acid nanoemulsion and conducted to ascertain the compatibility of drug with the surfactant and oil [12]. Azelic acid loaded nanoemulsion was frozen in liquid nitrogen and lyophilized. The coolant was liquid nitrogen [13]. Prior to heating, about 5 mg of each sample were subjected to an aluminium oxide pan with an empty pan used as a reference. DSC was set at 20 to 300 °C temperature range by scanning rate of 20 °C /min under the nitrogen atmosphere.

2.2.7.2 Thermogravimetric Analysis (TGA)

Thermo gravimetric analysis (TGA) is a crucial technique for studying the thermal stability and composition of materials. It used to characterize materials by measuring their changes in mass as a function of temperature; also helps identify decomposition temperatures, quantify composition, assess purity, and characterize crystalline and amorphous pharmaceutical materials. Thermo gravimetric analysis (TGA) of the optimized nanoemulsion was carried out using a TGA/SDTA851 (Mettler Toledo) instrument with a heating rate of 10 °C /minute in 150 µL alumina crucibles. This technique is used for measuring changes in the mass of the nanoemulsion that occur in response to temperatures ranging from 30 °C to 800 °C. Liquid nitrogen was used as a gas carrier in the system [14]. The sample was then loaded into the instrument in the aluminium pan and the empty pan was set as a reference.

2.2.8 Particle Size and Polydispersity Index (PDI) Determination

Droplet size of particles, and size distribution (PDI) in the nanoemulsion system were measured using dynamic light scattering, which scattered at an angle of 173° and a temperature of 25 °C. This process was carried out using a droplet size analyzer (Zetasizer Nano ZS90; Malvern Instruments, Malvern, UK). The

measurement of droplet size was done a day after the formulations were made to ensure that the system has achieved equilibrium. The required concentration of samples was obtained by diluting them with deionized water to reduce multiple scattering effects, before pouring them into a folded capillary cell [15]. The nanoemulsion particle size should be between 20–200 nm for cosmetic applications [16].

It is important to note that PDI indicates homogeneity and stability, wherein the target range should be lower than 0.5 for a nanoemulsion. This value shows similar and narrow size distribution in the Azelic acid formulation, representing a more stable and uniformed nanoemulsion system [17].

2.2.9 Zeta Potential

Zeta potential analysis is conducted to determine the surface charge of particles in a liquid, offering insights into colloidal stability, aggregation tendencies, and formulation optimization. Zeta potential values were obtained by using the particle size analyzer (Zetasizer Nano-ZS90, Malvern Instruments) through the technique of dynamic light scattering. The zeta potential was determined based on the measurement of the electrophoretic mobility of dispersed particles in a charged field. The samples were diluted in distilled water at a 1:20 ratio and placed in the equipment to be analyzed [18]. The analyses were performed in triplicate. At greater absolute values (more than +30 mV or less than –30 mV), the ZP of a system indicates the tendency of the particles to repel each other, which may indicate that the system is stable. If, however, the absolute values for the ZP are low or zero, the particles tend to agglomerate and the system can easily flocculate [19].

2.2.10 Field Emission Scanning Electron Microscopy (FESEM)

The morphology of the optimised azelic acid nanoemulsion was examined by using JHM-7600F FESEM (JOEL, Japan) according to the reported method [20]. It is apparatus that used for an image surface roughness analysis, used to explain the shape, size droplets within formulated azelic acid nanoemulsion.

2.2.11 Transmission Electron Microscopy (TEM)

Transmission Electron Microscopy (TEM) is a technique that uses an electron beam to image a nanoparticle sample, providing much higher resolution than is possible with light-based imaging techniques. TEM is the preferred method to directly measure nanoparticle size, size distribution, and characterize the droplet morphology of the optimized azelic acid formulation and investigated by using a transmission electron microscopy (TEM, JEOL JEM-1400Flash; JEOL, Tokyo, Japan). The sample was homogenized in deionized water. A formvar coated copper grid was added on top of a drop of diluted sample and left at room temperature (25 °C) for 3 min. The samples on the filled copper grid were then negatively stained using 2% w/w phosphotungstic acid for 2 min and air dried prior to analysis [21].

2.2.12 pH Measurement

The pH measurement is crucial to check the compatibility of a sample with human skin and evaluate the stability of emulsions, by monitoring pH throughout stability studies since variations in pH values suggest that chemical processes are taking place that may degrade the final product's quality [22].

The pH of the optimized azelic acid nanoemulsion was determined using a Delta 320 pH meter. An electrode with a glass membrane that is sensitive to hydrogen ions was used to measure the pH value. Prior to taking measurements, the pH meter was calibrated with three standard buffer solutions (pH 4.00, 7.00 and 10.00) [23]. The pH value was determined by the direct insertion of the electrode into the sample. The measurements of the pH of the formulation were performed in triplicate and the average values were calculated. The pH of skin is around 5.5 and often a pH in the range of 4.0 to 7.0 is suitable for topical application. So, pH of the formulation needs to be within this range to be compatible with human skin [24].

2.2.13 Viscosity

Viscosity plays an important role in the delivery of drugs used via topical or transdermal application. Several characteristics of formulations including the stability, spread ability, drug release, absorption of drug across the skin and ease of application are dependent on the viscosity [25]. Viscosity is defined as the shear stress divided by the rate of shear strain [26]. The viscosity of the optimized nanoemulsion was determined using a rheometer (TA Instruments, New Castle, DE, USA). The measurement was carried out with 4 °C/40 mm cone and plate geometries (gap of 0.100 mm) at 25 °C. The steady rheological behavior of the sample was analyzed at a controlled rate varying from 0.1 to 100 s⁻¹. The sample was allowed to stand for 10 min to achieve an equilibrium state prior to measurement. The experimental data were fitted to the power-law model as in Equation (2):

$$\eta = ky^{n-1} \dots \dots \dots (2)$$

Where η is the viscosity (Pa.s); $\dot{\gamma}$ is the shear rate (s^{-1}); and k and n are the consistency index and flow behaviour index, respectively. A desirable nanoemulsion with pseudo-plastic behaviour is more preferable for topical application.

2.2.15 Stability Study

The stability of nanoemulsion is defined by the capability of the formulation (in a specific system) to maintain its physical appearance, without any phase separation or physical changes over a specific time of storage and during use.

This study's stability tests were simulated under conditions that are likely to destabilize the azelic acid nanoemulsion over time. The azelic acid nanoemulsion was subjected to three stability studies; stability under a centrifugation test, storage stability at different temperatures (- 5, 25 and 40°C) for 7 weeks and freeze-thaw cycles, as well as under conditions of high heat and cold. The stability of the azelic acid nanoemulsion was determined through the visible appearance of creaming or phase separation, pH, and viscosity, were recorded before each test [27].

To test its stability under a centrifugation test, the azelic acid nanoemulsion was kept in a centrifuge tube and was subjected to centrifugation force at 4000 rpm for 15 minutes. The azelic acid nanoemulsion was then observed for any phase separation or physical change. To determine its storage stability at different temperatures (- 5, 25 and 40°C), the azelic acid nanoemulsion was observed in terms of its physical appearance on 1, 2, 3, 4, 5, 6 and 7 weeks of storage time.

The freeze-thaw cycle test was done for temperatures -4 °C (in the freezer), followed by room temperature (\pm 25 °C) at 24 h intervals, by subjecting each sample to a triple repeated cycle of freezing and thawing. Each condition was maintained for 24 h before the condition was changed. The physical appearance of an adequately stable azelic acid nanoemulsion post-evaluation test should be similar to the pre-evaluated one and without any phase separation [28]. The pH stability of the azelic acid nanoemulsion was then measured at - 4, 25 and 40°C after a 6-week incubation.

2.2.17 Drug content & Encapsulation Efficiency (EE)

Drug content of the nanoemulsion formulation was carried out by dissolving 1 ml of the formulation in 10 ml of methanol, to extract the entrapped azelic acid in the prepared nanoemulsion formulations. This formulation was then placed in shaking incubator (50 rpm) for 30 min. After 30 min by centrifugation, the supernatant was collected and filtered. The sample was analysed at 269 nm using UV-VIS spectroscopic method after making suitable dilutions against methanol as a blank [29].

Azelic acid content represents the total amount of azelic acid in the formulation, whereas the entrapment efficiency represents the amount of azelic acid inside the nanometric droplets. The drug solubility and compatibility with the oil phase and the excipients used in the preparation of the formulations have a great impact on the entrapment efficiency and drug content values [30]. Azelic acid content was determined by analysing filtrate using UV-VIS spectroscopic method.

Percentage entrapment efficiency was calculated using the equation (3):

$$\% \text{ Drug entrapment efficiency} = \frac{\text{Total amount of drug} - \text{amount of unbound drug}}{\text{Total amount of Drug}} \times 100 \dots\dots(3)$$

2.2.18 In-vitro release studies

In vitro release kinetics of azelic acid -nanoemulsion and azelic acid emulsion were evaluated by the dialysis membrane. The release studies were done in 0.2 M phosphate buffer as the dissolution medium with pH 7.4 (receptor compartment). The 1ml azelic acid -nanoemulsion (equivalent to 10000 $\mu\text{g/ml}$) and azelic acid emulsion formulation placed in a dialysis membrane and sealed at both ends. Then the dialysis membrane containing azelic acid -nanoemulsion as donor compartment, was immersed in the receptor compartment (containing 50 ml of the dissolution medium) and it was stirred using magnetic stirrer at 100 rpm and maintained at 32 ± 0.5 °C. About 2ml aliquots were withdrawn at predetermined time intervals (0, 0.25, 0.5, 1, 2, 4, 6, 8 and 12 h) and replaced with fresh media of similar volume. The cumulative amount of azelic acid released in the dissolution medium was determined by UV-visible spectrophotometer method (λ_{max} of azelic acid: 204 nm) [31]. The release rate of azelic acid from azelic acid - nanoemulsion was compare with azelic acid - emulsion. Cumulative amount of drug release was calculated using below equation

$$\% \text{ Drug Release} = \frac{\text{Con.} \left(\frac{\mu\text{g}}{\text{ml}} \right) \times \text{vluem of release medium (ml)} \times \text{dilution factor}}{\text{intial amount of drug taken } \mu\text{g}} \times 100 \dots\dots\dots(5)$$

2.2.18 Kinetic Release Study

The linear regression analysis of the data obtained from the *in vitro* release study in mathematical models was conducted to determine the release kinetics of the azelic acid from its system. The mathematical models were zero-order (cumulative amount of drug release against time, Equation (4)), first-order (log cumulative amount of drug remaining against time, Equation (5)), Higuchi (cumulative percentage of drug release against square root of time, Equation (6)), Hixson-Crowell (cube root cumulative amount of drug remaining against time, Equation (7)) and Korsmeyer-Peppas (log cumulative percentage of drug release against log time, Equation (8)) [32]. The model that showed the highest coefficient determination (R^2) was chosen as the best model that fitted the data obtained from the release study. The theoretical equations for each model that were used to plot the graph were shown below.

$$M_t = M_0 + K_0t \dots\dots\dots(6)$$

$$\log M_t = \log M_0 + K_1t/2.30 \dots\dots\dots(7)$$

$$Q = K_H \times t^{1/2} \dots\dots\dots(8)$$

$$M_0^{1/3} - M_t^{1/3} = K_{HC} t \dots\dots\dots(9)$$

$$M_t/M_\infty = K_{kp}t^n \dots\dots\dots(10)$$

where M_0 is the initial amount of azelic acid in dissolution media, M_t is the amount of azelic acid released in time t , M_∞ is the amount of drug released after time ∞ , K_0 , K_1 , K_H , K_{HC} and K_{kp} are the release rate constants, Q is the cumulative amount of azelic acid released in time t per unit area, fraction of azelic acid release over time, n is the release exponent and t is the time.

2.2.19 Ex-Vivo Permeation studies

For this test, we used pig ear skin from a slaughterhouse immediately after slaughter of the animal and an automatic Franz diffusion cell (Logan instrument Corporation, NJ USA). For ex vivo skin penetration studies the OECD guideline recommends pig ear skin as suitable skin surrogate to mimic human percutaneous penetration. Pig ear skin shows similarities in morphology as well as penetration abilities and corresponds to that of human skin [33-36].

The ears were cleaned with water (32 ± 0.5 °C), and the ears with injuries were discarded. The undamaged skins were removed from the cartilage with a scalpel, and adipose tissue, adhering lipid subcutaneous layer, extraneous debris and leachable enzymes of the skin samples were removed. On the day of the experiment, the skin was thawed in a phosphate buffer solution, pH 7.4 at 32 ± 0.5 °C for 30 min. Pig skins were mounted on Franz diffusion cells and 1ml of optimized azelic acid -nanoemulsion (equivalent to 10000 µg/ml) or azelic acid emulsion was placed on the surface of the skin in the donor phase. About 11 ml of phosphate buffer (0.2M, pH 7.4) as the receptor media (constantly stirred at 600 rpm for 8 h at 32 ± 0.5 °C). The skin surface temperature was maintained at 32 °C to approximate normal skin conditions by thermostatic water pump during the experiment. The samples (approximately 2 ml) of receptor medium were withdrawn at pre-determined time intervals (0, 0.25, 0.5, 1, 2, 4, and 8 h) and then immediately replaced with an equal volume of medium heated to 32 °C. The permeated azelic acid was determined in samples using a spectrophotometer analysis at 204 nm [37,38].

2.2.20 Skin Retention

During the retention studies, the azelic acid remaining was evaluated using solvent extraction. After 24 h towards the end of study, the skin fragments were removed from the diffusion Franz cells for evaluation of drug remaining in skin samples. The remaining substances of skin surface were removed via three times washing with PBS, pH 7.4. The samples sliced into small segments and then samples were placed in a buffer solution and sonicated for 1 h using a bath sonicator. The obtained supernatants from this stage were collected and filtered by 0.22 µm membrane. At the end of the experiment, the amounts of drug remaining in the skin were quantified using a spectrophotometer analysis at 204 nm [39,40].

3. Results & Discussion

3.1 Selection of the Nanoemulsion Components

The selection of the nanoemulsion components is one of the most important steps of the formulation development, was performed during the initial pre-formulation studies. The most suitable oil, surfactant and co-surfactant were selected by analysing solubility of azelic acid in different components. The solubility of azelic acid in different oily phases, surfactants and co-surfactants were determined. The solubility of carvedilol was found to be highest in castor oil (1.90 ± 0.06 mg/ml) and Vitamin E (1.67 ± 0.08 mg/ml) in comparison to peppermint oil in table 3.1. Hence, castor oil and vitamin E were selected as the oil phase.

High drug solubility was found in Tween 80 (52.09%) among surfactants and in Transcutol P (40.03%) among co-surfactants in table 3.2. Therefore, based on the solubility and potential of emulsification, Castor oil and vitamin E was selected as the oil phase, Tween-80 were selected as surfactants and Transcutol P were selected as co-surfactants, respectively, for the development of Nanoemulsion.

Table 3.1: Solubility study in oil

S. No	Oils	Solubility mg/ml
1	Peppermint oil	0.22 ± 0.02
2	Vitamin E	1.67 ± 0.08
3	Castor oil	1.90 ± 0.06

Table 3.2: The present transmittance of surfactant and co-surfactant

S. No	Surfactant	% Transmittance
1	Transcutol P	40.03
2	Poloxamer 188	15.30
3	Poloxamer 407	19.89
4	Tween 80	52.09

3.2 Formulation optimization using Box-Behnken design

According to the Box–Behnken design 17 Azelic acid nanoemulsion formulations were developed by emulsification ultra-sonication method and investigated to determine the effect of independent variables on dependent variable. The observed values of the three responses viz. particle size, PDI and % entrapment efficiency for all batches. The selected independent variables were found to influence the three responses measured. From the experimental results, it is observed that all batches showed particle size in the range between 170 and 276 nm, PDI 0.2 to 0.7 and % EE 50-85.84 %. Hence F2 was considered as optimized formulation because according to previously discussed criteria only the formulation no. 02 provided lowest globule size 184 nm, lowest PDI 0.2 and maximum entrapment efficiency 85.84 %. This optimized batch and subjected to further characterization studies.

3.3 Analysis of data using Box–Behnken design

3.3.1 Effect of independent factors on particle size

Particle size is an important variable for assessing the nanoemulsion. Smaller the particle size larger will be the interfacial surface area for drug absorption. The model F-value of 188.95 implies the model is significant. There was only a 0.01% chance that an F-value this large could occur due to noise. P-values less than 0.0500 indicate model terms are significant. In this case A, B, AC, BC, A², B² are significant model terms. R² value was 0.9007, which indicate that the model is significant. The predicted R² of 0.8344 is in reasonable agreement with the adjusted R² of 0.9007; i.e. the difference is less than 0.2. Adequate precision measures the signal to noise ratio. A ratio greater than 4 is desirable. A ratio of 39.898 indicates an adequate signal.

Table 3.3: Fit Summary of Particle size

Sr. No.	Source	Sequential p-value	Lack of fit p-value	Adjusted R ²	Predicted R ²	
1	Linear	0.00076	-	0.3342	0.2134	-
2	2 F1	0.4235	-	0.5336	-0.2910	-
3	Quadratic	< 0.0001	-	0.9007	0.8445	Suggested
4	Cubic		-	1.0000		Aliased

Table 3.4: ANOVA for Quadratic model of particle size

Sr. no.	Source	Sum of Squares	Df	Mean Square	F-value	p-value	
1	Model	19487.12	9	2253.70	190.34	<0.0001	significant
2	A-PVA: Xanthan gum	11034.09	1	11034.09	970.43	<0.0001	-
3	B-Tween 80: Transcutol P	172.32	1	172.32	16.02	0.0061	-
4	C- Homogenization speed	41.25	1	41.25	3.60	0.1043	-
5	AB	0.2600	1	0.2600	0.0220	0.8865	-

6	AC	842.00	1	842.00	74.83	<0.0001	-
7	BC	362.00	1	362.00	32.78	0.0008	-
8	A ²	6230.09	1	6230.09	540.00	<0.0001	-
9	B ²	561.02	1	561.02	50.88	0.0002	-
10	C ²	0.0669	1	0.0669	0.0059	0,9543	-
11	Residual	80.67	7	12.89	-	-	-
12	Lack of fit	80.67	3	27.42	-	-	-
13	Pure Error	0.0000	4	0.0000	-	-	-
14	Cor Total	19642.99	16				

The mathematical relationship in the form of a polynomial equation for the measured response (globule size), Y1, is mentioned below (Eq. 13):

$$\text{Particle Size (Y1)} = +186.00 + 38.12 A + 4.62 B - 3.256C - 0.2600 AB - 14.53 AC - 9.52 BC + 38.14 A^2 + 11.65 B^2 - 0.1251 C^2 \dots\dots\dots(13)$$

The positive values are related with synergistic effects (optimization) while the negative values are related with inverse/antagonistic effects in these regression equations 13, 14, & 15. It was observed that on increasing the PVA: Xanthan gum ratio, the size of the azelic acid emulsion increased. This effect could be attributed to the fact that in nanoemulsion formulation, by increasing the solid content, the dispersion viscosity also increases that result into higher surface tension and thus higher particle size. This effect was also promoted by increasing the Tween 80: Transcutol P ratio in the formulation. The particle size was decreased by increasing the homogenization speed in the formulation. The response surface analysis plots in three-dimensional model graphs obtained for globule size is shown in Fig. 3.1. These plots were used to study the interaction effects of two independent variables on the responses while holding the third factor at a constant level.

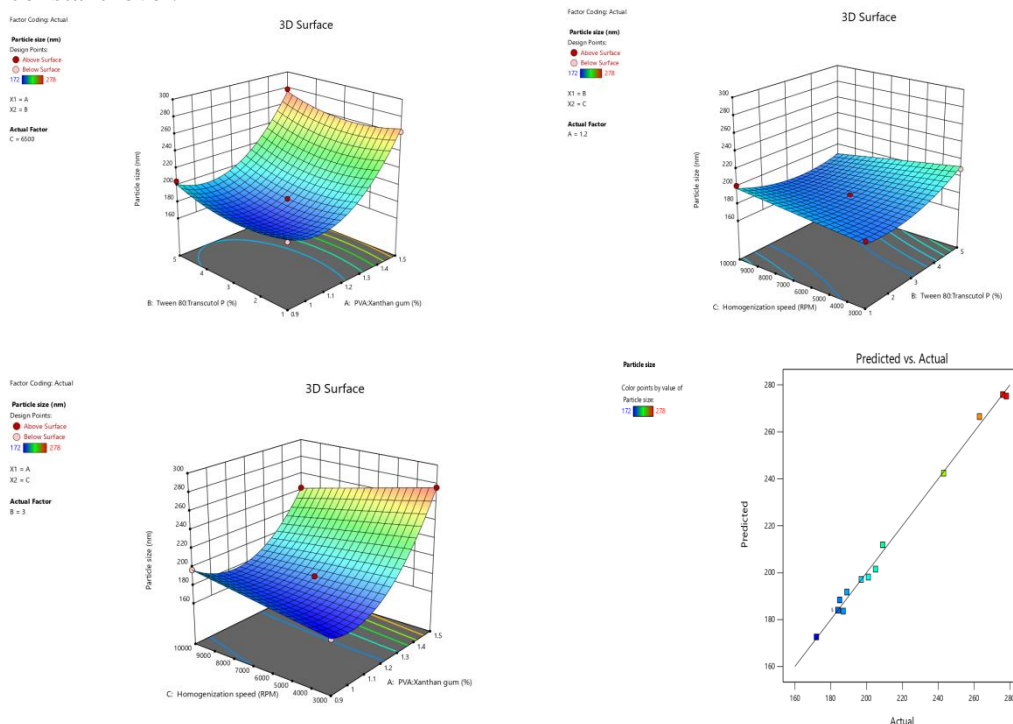


Figure 3.1: Response surface analysis plots for particle size and predicted Vs actual plot of particle size

3.3.2 Effect of independent factors on polydispersity index

The polydispersity index is a ratio that furnishes information about the homogeneity of the particle size distribution in a given system. The polydispersity index showed (Table 3.5) that all the nanoemulsions have narrow size distribution. The model F-value of 299.18 implies the model is significant. There is only a 0.01% chance that an F-value this large could occur due to noise. P-values less than 0.0500 indicate model terms are significant. In this case A, C, AB, AC, BC, A², B², C² are significant model terms. Values greater than 0.1000 indicate the model terms are not significant. The predicted R² of 0.9699 is in reasonable agreement with the adjusted R² of 0.9950; i.e. the difference is less than 0.2. R² value was 0.9950, which indicate that the model

is significant. Adequate precision measures the signal to noise ratio. A ratio greater than 4 is desirable. A ratio of 55.195 indicates an adequate signal.

Table 3.5: Fit Summary of PDI

Sr. No.	Source	Sequential p-value	Lack of fit p- value	Adjusted R ²	Predicted R ²	
1	Linear	0.4843	-	-0.0219	-0.4231	-
2	2 F1	0.3888	-	0.0099	-0.4509	-
3	Quadratic	< 0.0001	-	0.9950	0.9699	Suggested
4	Cubic		-	1.0000		Aliased

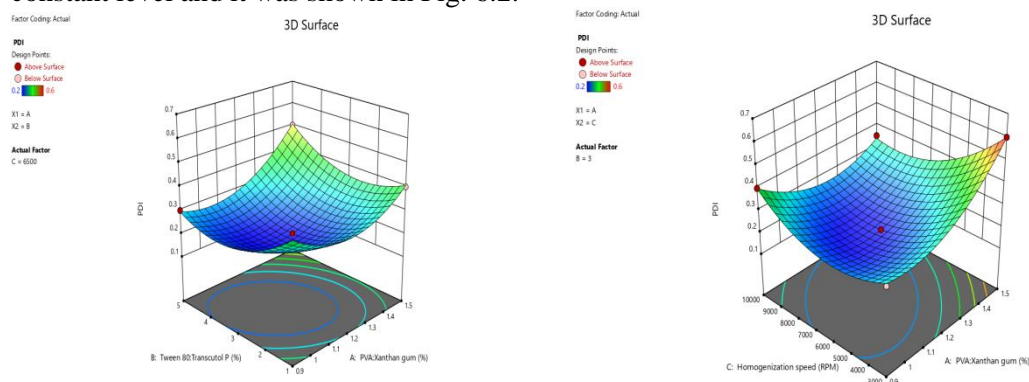
Table 3.6: ANOVA for Quadratic model of PDI

Sr. no.	Source	Sum of Squares	Df	Mean Square	F- value	p-value	
1	Model	0.2499	9	0.0265	299.18	<0.0001	significant
2	A-PVA: Xanthan gum	0.0265	1	0.0265	285.52	<0.0001	-
3	B-Tween 80: Transcutol P	0.0000	1	0.0000	0.0000	1.0000	-
4	C- Homogenization speed	0.0165	1	0.0165	172.55	<0.0001	-
5	AB	0.0100	1	0.0100	112.00	<0.0001	-
6	AC	0.0407	1	0.0407	344.00	<0.0001	-
7	BC	0.0100	1	0.0100	112.00	<0.0001	-
8	A ²	0.0576	1	0.0576	534.40	<0.0001	-
9	B ²	0.0472	1	0.0472	121.34	<0.0001	-
10	C ²	0.0480	1	0.0480	540.23	<0.0001	-
11	Residual	0.0007	7	12.89	0.0001	-	-
12	Lack of fit	0.0007	3	0.0003	-	-	-
13	Pure Error	0.0000	4	0.0000	-	-	-
14	Cor Total	0.2399	16		-	-	-

Quadratic equation generated for effect on PDI is as follows:

$$\text{Response 2 PDI (Y2)} = +0.3003 + 0.0587 A + 0.0000 B - 0.0423 C + 0.0500 AB - 0.0879 AC + 0.0500 BC + 0.1076 A^2 + 0.0976 B^2 + 0.1089 C^2 \dots\dots\dots(14)$$

PDI is an important parameter indicating the stability of nanoemulsion. Theoretically, lower PDI values stabilize the particle nanoemulsion. The results of Box-Behnken design suggested that as PVA: Xanthan gum increased, PDI also increased while Tween 80: Transcutol P (C) had negligible effect on PDI. We ascertain that an increased Homogenization speed leads to decrease in polydispersity index of nanoemulsions at a certain level. The response surface analysis plots in three-dimensional model graphs were constructed for PDI, to study the interaction effects of two independent variables on PDI while holding the third factor at a constant level and it was shown in Fig. 6.2.



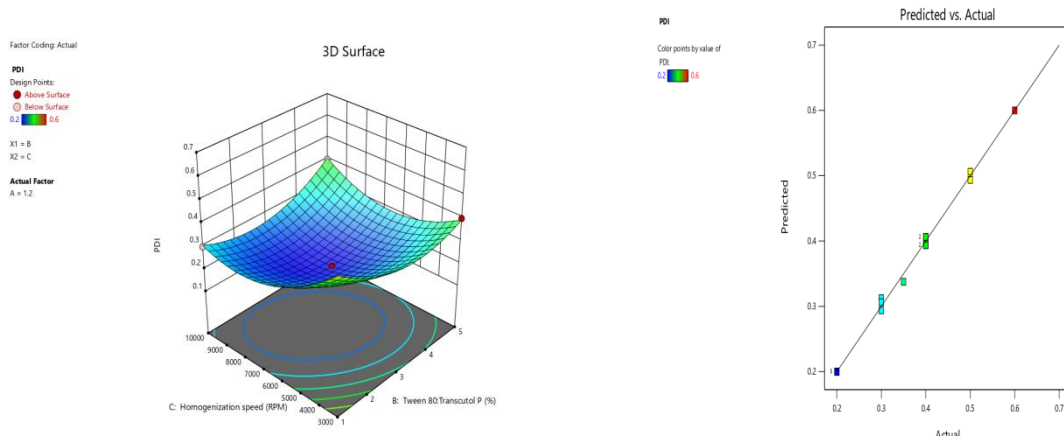


Figure 3.2: Response surface analysis plots for PDI and predicted Vs actual plot of PDI

3.3.3 Effect of independent variables on Entrapment Efficiency (Y3)

The model F-value of 136.15 implies the model is significant. There is only a 0.01% chance that an F-value this large could occur due to noise. P-values less than 0.0500 indicate model terms are significant. In this case A, B, C, AB, AC, BC, A², B², C² are significant model terms. The predicted R² of 0.9195 is in reasonable agreement with the adjusted R² of 0.9970; i.e. the difference is less than 0.2. R² value was 0.9970, which indicates that the model is significant. Adequate precision measures the signal to noise ratio. A ratio greater than 4 is desirable. A ratio of 34.424 indicates an adequate signal. This model can be used to navigate the design space.

Table 3.7: Fit Summary of % EE

Sr. No.	Source	Sequential p-value	Lack of fit p- value	Adjusted R ²	Predicted R ²	
1	Linear	0.8485		-0.1670	-0.4231	-
2	2 F1	0.5422		-0.02230	-0.4509	-
3	Quadratic	< 0.0001		0.9970	0.9195	Suggested
4	Cubic			1.0000		Aliased

Table 3.8: ANOVA for Quadratic model of % EE

Sr. no.	Source	Sum of Squares	Df	Mean Square	F- value	p-value	
1	Model	2145.88	9	237.89	136.15	<0.0001	Significant
2	A-PVA: Xanthan gum	22.11	1	22.11	13.01	0.0097	
3	B-Tween 80: Transcutol P	13.03	1	13.03	8.60	0.0097	-
4	C- Homogenization speed	92.90	1	92.90	55.40	0.0003	-
5	AB	100.00	1	100.00	60.67	0.0001	-
6	AC	242.30	1	242.30	144.78	<0.0001	-
7	BC	26.00	1	26.00	15.90	0.0063	-
8	A ²	782.80	1	782.80	461.78	<0.0001	-
9	B ²	690.34	1	690.34	412.44	<0.0001	-
10	C ²	37.90	1	37.90	22.99	0.0023	-
11	Residual	12.80	7	1.98	0.0001	-	-
12	Lack of fit	12.80	3	4.01	-	-	-
13	Pure Error	0.0000	4	0.0000	-	-	-
14	Cor Total	20987	16	-	-	-	-

The effect of independent variables on %EE could be quantified by the following quadratic equation-

$$\% EE(Y3) = +84.90 -1.66 A -1.29 B -3.33 C -5.00 AB -7.77 AC -2.59 BC -13.53 A^2 -12.80 B^2 +2.99 C^2 \dots\dots\dots(15)$$

The increase in the PVA: Xanthan gum and tween 80: Transcutol P showed entrapment efficiency decreased. Moreover, increasing amount of homogenization speed leads to decreased entrapment efficiency. Increased tween 80: Transcutol P and homogenization speed showed less effect as compared to PVA: Xanthan gum. The response surface plots (Figure 6.3) showed the effects of all three factors on entrapment efficiency.

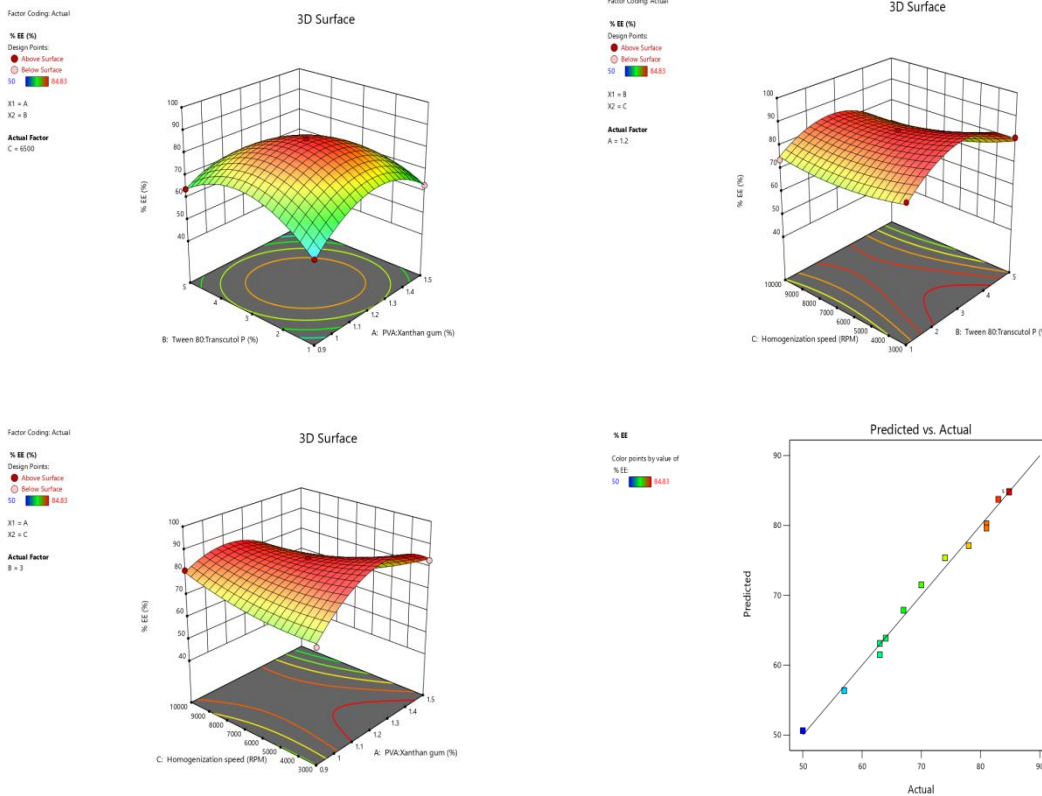


Figure 3.3: Response surface analysis plots for entrapment efficiency and predicted Vs actual plot of entrapment efficiency

3.3.4 Fourier Transform Infrared (FTIR) Analysis

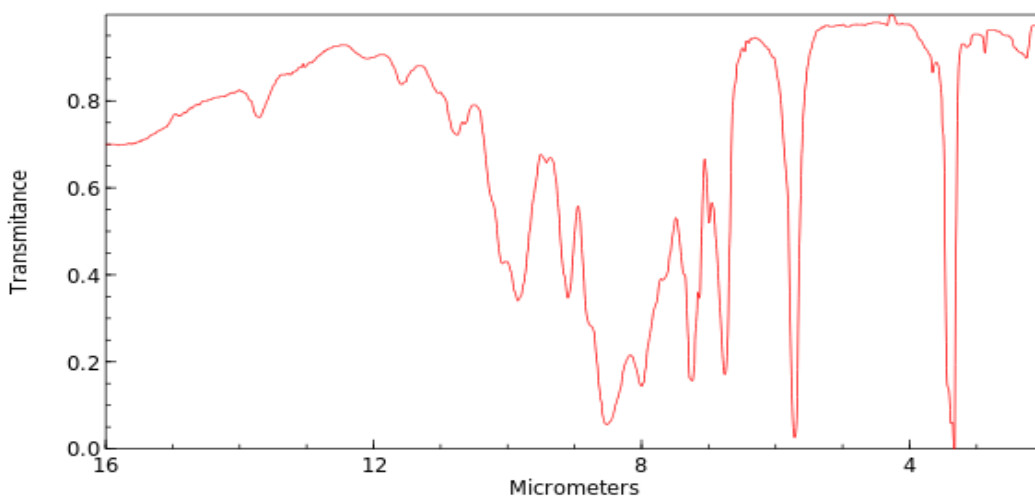


Figure 3.4: FTIR of azelic acid nanoemulsion

Table 3.9: FTIR interpretation of Azelic acid Nanoemulsion

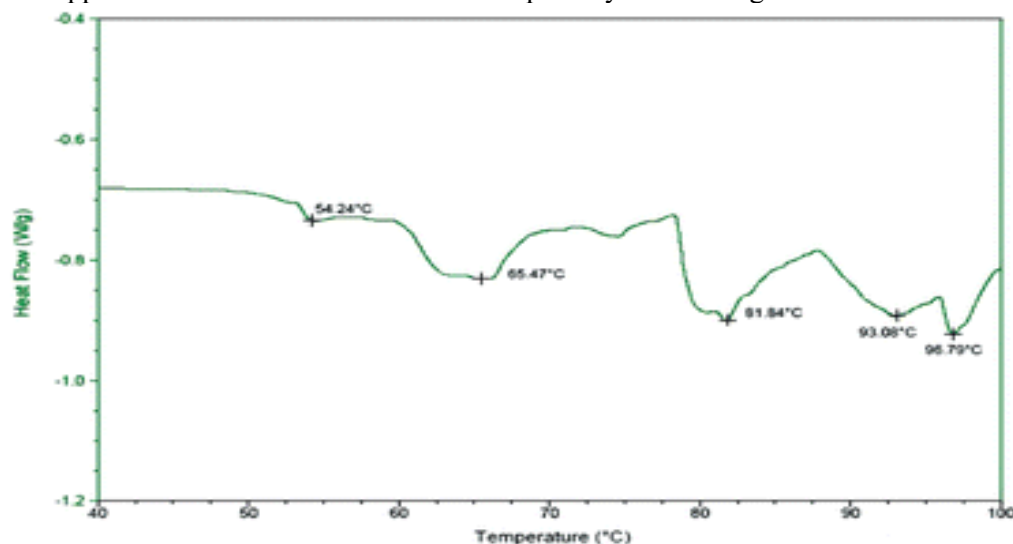
Characteristics Peaks	Reported (cm ⁻¹)	Observed (cm ⁻¹)
axial deformation of an alcoholic (-OH) hydroxyl groups	3200–3500	3338.99
C=O stretching	1635.83	1638.8
C–H stretching vibration	2965, 2889	2960, 2808
the C ₄ -C ₅ stretch	1475	1465.2

FTIR spectrum of the azelic acid nanoemulsion was shown in Figure 3.4. The FTIR spectrum of azelic acid nanoemulsion revealed, characteristic peak at 3338.99 cm⁻¹ shows the presence of C–O group of azelic acid; 2985 cm⁻¹ and 2810 cm⁻¹, related to stretching vibration of C–H bonds, and peak 1465.2 cm⁻¹ belongs to C₄–C₅ stretching of azelic acid. While peak at 3333.2 cm⁻¹ is characteristic of axial deformation of an alcoholic (-OH) hydroxyl groups of Xanthan Gum and O–H stretching arising from the intermolecular and intramolecular hydrogen bonds of PVA. In addition, the band at 1656 cm⁻¹, related to stretching vibration of C = O of free azelic acid shifted 1639.3 cm⁻¹ in azelic acid nanoemulsion. This shifting was due to the loading of azelic acid and binding with polymers by hydrogen bonds. The above data and appearance of azelic acid bands in azelic acid nanoemulsion confirms the loading of azelic acid in the Azelic acid nanoemulsion.

3.4 Thermal Analysis

3.4.1 Differential Scanning Calorimetry (DSC)

DSC analysis was used to characterize the enthalpy changes and melting temperature and recrystallization behaviour, unloaded and loaded nanoparticles. DSC thermogram of azelic acid nanoemulsion has shown in the Figure 3.5. Azelic acid -nanoemulsion had small endothermic peaks at 145.28 °C and 201.68 °C. The melting endotherm of PVA and Xanthan gum was completely absent in the thermo grams of azelic acid -nanoemulsion structure and the melting peak of both might overlapped and formation of a new peak was observed at 201.68 °C [235]. The depression of melting temperature indicates that the crystallization process of the two polymers was hindered due to interactions between the functional groups of polymers. The PVA exhibits two broad decomposition endothermic peaks at around 322.36 °C and 378.15 °C probably due to PVA inducing water evaporation phase. The melting endotherm of the azelic acid at 158.6 °C was reduced to 145.28 °C in the thermo grams of azelic acid -nanoemulsion structure, which indicates a decrease in degree of crystallinity. The decrease in crystallinity of azelic acid corresponded with the increase in azelic acid entrapped in azelic acid nanoemulsion amorphously and in a high amount.

**Figure 3.5: DSC of azelic acid nanoemulsion**

3.4.2 Thermo gravimetric Analysis (TGA)

TGA have been widely used to evaluate the thermal properties of materials and to show the mechanism by which a material loses weight as a result of controlled heating. Figure 3.6 presents the curves corresponding to the mass loss of azelic acid nanoemulsion as a function of temperature. In the TGA thermogram of Azelic acid nanoemulsion, weight loss occurred in three distinct transformation regions in the system. In the first region of mass loss, the azelic acid nanoemulsion shows weight loss of 32.3% between 28 and 80 °C

temperature range, which may be due to the removal of the continuous phase (deionized water) in the nanoemulsion? In the second region, a significant weight loss was noticed in the temperature range of 90.03°C–345.55°C. The greater loss of mass of the azelic acid nanoemulsion was observed, which can be attributed to decomposition temperature due to the presence of azelic acid drug. At very high temperatures, 6.30% of the residue was left and was completely decomposed at 494.90°C. This could be because of the decomposition process of oil occurring during the combustion of organic-bound carbon in the oil. The result of TGA thermal analysis confirms the incorporation of azelic acid in the structure of Azelic acid nanoemulsion.

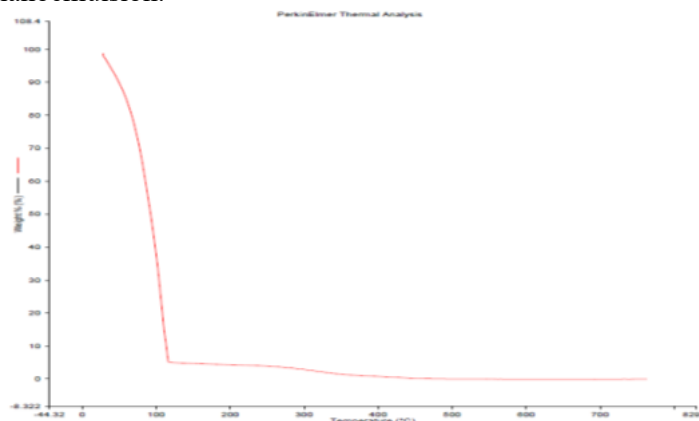


Figure 3.6: TGA of Azelic acid nanoemulsion

3.5 Particle Size and Polydispersity Index (PDI) Determination

Results revealed that azelic acid nanoemulsion have a droplet size of 184 nm, and a polydispersity index (PDI) 0.202. For cosmeceutical purposes, the nanoemulsion with a droplet size ranging between 100 to 200 nm was more favourable. The droplet size of 184 nm indicated that the azelic acid formulation would have better penetration of the azelic acid into the skin layers. Polydispersity (PDI) analyses the size distribution, demonstrating the uniformity of the droplet size. The good monodisperse system should have a PDI value lower than 0.5 or lower than 0.30. As the PDI value of the azelic acid formulation was 0.202, this indicated a good monodisperse system and is expected to be a stable emulsion. The mean particle size based on the TEM image was 200 nm, which was in-consistent with the size measured by DLS but correlates with the range of droplet diameter obtained from DLS.

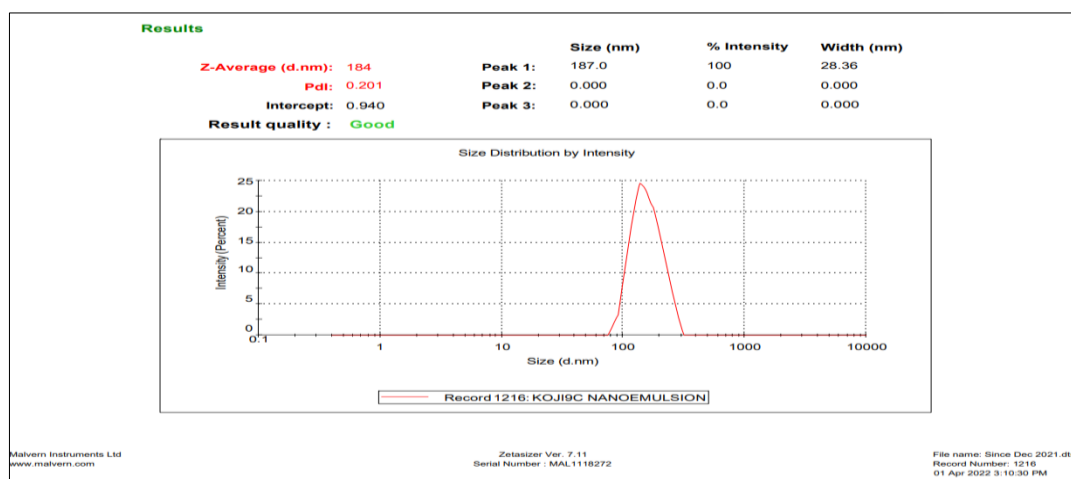


Figure 3.6: Particle size & PDI of Azelic acid nanoemulsion

3.4.4 Zeta Potential

The zeta potential of the optimized nanoemulsion containing azelic acid was found to be -35.90 mV. The zeta potential measures the electro kinetic potential of a particle and used to determine the stability of the nanoemulsion. The formulation is considered stable when the value is more than $+25$ mV or lowers than -25 mV. The azelic acid formulations with a zeta potential value of -35.90 mV demonstrated a higher electrostatic repulsion, which indicated that the nanoemulsion system was stable.

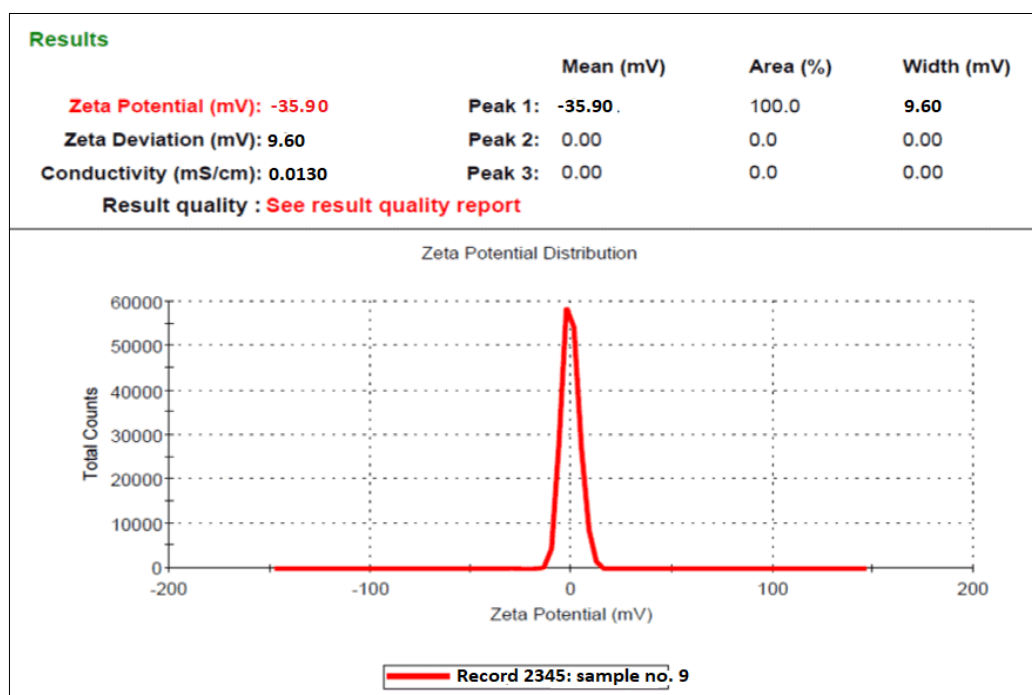


Figure 3.7: Zeta potential of Azelic acid nanoemulsion

3.4.5 Field Emission Scanning Electron Microscopy (FESEM)

Optimised azelic acid nanoemulsion was viewed under FESEM. Surface morphology of nanoparticles is shown in figure 3.8. FESEM image revealed that experimental formulations displayed small spherical shaped particles with uniformity and most of the particles were below 500 nm in size. There were no large cluster and no significant changes in the droplet size and shape were observed in the formulation, which indicated that the optimised emulsifier concentration and processing conditions obtained in the study had successfully produced homogeneous and uniform azelic acid nanoemulsion formulation.

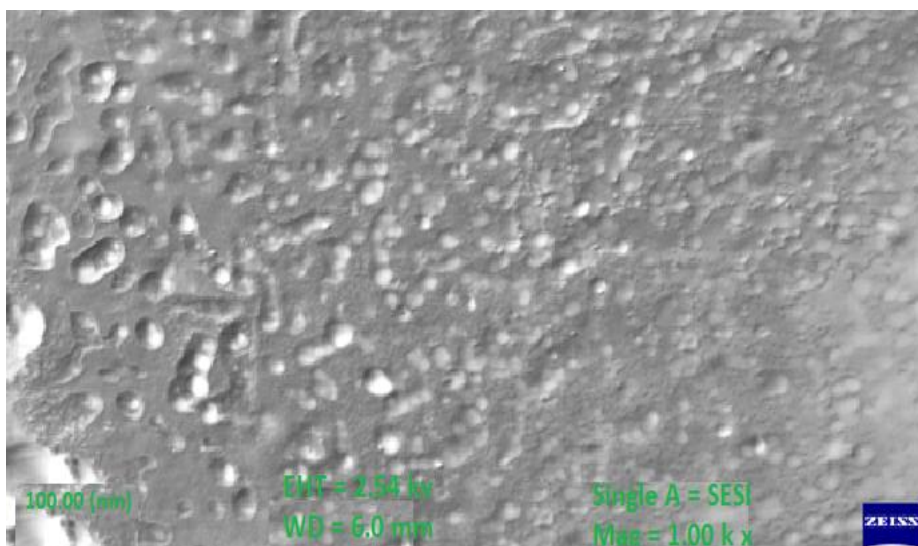
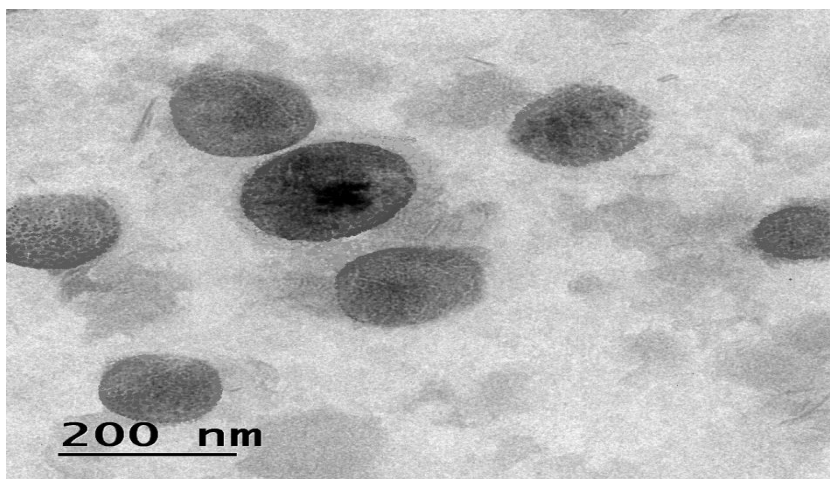


Figure 3.8: FE-SEM image of Azelic acid nanoemulsion

3.4.6 Transmission Electron Microscopy (TEM)

Morphology of nanoemulsion was visualized and characterized by transmission electron microscopy (TEM). Figure 3.9 shows the TEM image of azelic acid nanoemulsion. The droplets were spherical shaped in morphology. The particle size obtained was 200 nm. The mean particle size measured by DLS was 184 nm, which was in-consistent with the size based on the TEM image. But the data pertaining to droplet size obtained by TEM analysis correlates with the range of droplet diameter obtained using particle size analyser (DLS).



Figures 3.9: TEM images of Azelic acid nanoemulsion

3.4.7 pH Measurement

For topical applications, the pH range between 4.0 to 7.0 is preferable because it should closely resemble the pH of the surface of healthy human skin and should be compatible with human skin. The pH value of the Azelic acid nanoemulsion was observed 5.62, which was found to be within the above-mentioned pH range, indicating its suitability for use as a topical formulation.

3.4.8 Viscosity

The viscosity of the azelic acid nanoemulsion was determined by utilizing Brookfield cone and plate viscometer. The viscosity of the Azelic acid loaded nano-emulsion was observed 128 cps which might be attributed to the o/w nature of the nanoemulsion. The viscosity of the Azelic acid formulation was decreased due to the small droplet diameter. The optimized azelic acid loaded nanoemulsion exhibits non-Newtonian pseudo-plastic behaviour and was suitable for the topical delivery. This semi viscosity of the nano emulsion is expected to provide increased retention of the formulation at the skin with controlled release of entrapped medication to obtain its therapeutic efficacy and stability toward phase separation.

3.4.9 Stability Study

Stability is one of the important parameter for nanoemulsion. A nanoemulsion should remain physically stable throughout its shelf life with no or minimal changes in the particle size. The azelic acid nanoemulsion showed no physical changes or phase separation after being subjected to centrifugation test and freeze-thaw cycle test. This test is also useful for predicting the prepared Azelic acid nanoemulsion's shelf life under storage normal conditions. The absence of phase separation in the sample confirms the stability of the nanoemulsion system.

Table 3.10: Thermo stability test results on phase separation for Azelic acid nanoemulsion (centrifugation test and freeze-thaw cycle test)

Tests	Phase separation
freeze-thaw cycle test	No
centrifugation test	No

/ = stable or no physical changes

A storage stability study was carried out by stored Azelic acid nanoemulsion at three different temperatures (5, 25 and 40°C) for 7 weeks. Table 6.13 showed that the azelic acid nanoemulsion remained a homogenous mixture and no physical or phase changes were observed in the first 6 weeks under all storage temperatures. 3 samples of optimized azelic acid nanoemulsion which were subjected to extended storage at the lowest temperature (5°C) and room temperature (25°C) appeared whiter in colour and no phase changes were observed. Azelic acid formulation was slightly yellowish when stored at the highest tested temperature (40°C) after 6 weeks. Hence, the formulations produced here were not suitable for storage at temperatures exceeding 35-37 °C.

Table 3.11: Storage stability test results on phase separation for azelic acid nanoemulsion under different storage temperatures

TEMP	Week 1	Week 2	Week 3	Week 4	Week 5	Week 6	Week 7
5°C	NPC						
25°C	NPC						
40°C	NPC	NPC	NPC	NPC	NPC	NPC	PC

NPC=stable or no physical changes; PC = not stable or physical changes observed

3.3.10 pH Stability over an Extended Storage Period

In this research, the pH of azelic acid nanoemulsion was determined by using pH meter weekly for 7 weeks, and they were found to range between pH 4.66 to 5.19. All formulations generally showed a decreasing trend in terms of pH value from week 1 to 7 week. This can be attributed to the presence of free fatty acids liberated by the degradation of the oil phase components or the hydrolysis process caused by the temperature factor.

Table 3.12: Storage stability for pH

TEMP	Week 1	Week 2	Week 3	Week 4	Week 5	Week 6	Week 7
5°C	5.30	5.33	5.34	5.50	5.56	5.32	4.66
25°C	5.99	5.98	5.76	5.43	5.67	4.90	4.83
40°C	5.97	5.86	5.86	5.37	5.50	4.86	5.19

3.3.11 Drug Content & Encapsulation Efficiency (EE)

The prepared Azelic acid loaded nanoemulsion formulations exhibited drug content value 96.25 ± 0.40 % and indicated that the drug had been precisely loaded into the formulation and had little degradation and few handling errors. The entrapment efficiency of azelic acid nanoemulsion was obtained 84.92 ± 2.6 %. The present study depicted good agreement between the drug compatibility and the oil phase and the excipients used in the preparation of the Azelic acid -loaded nanoemulsion formulations.

3.3.12 In-vitro release studies

An in vitro release study was carried out to study in vitro drug release profile of the azelic acid nanoemulsion and to compare the release pattern of the azelic acid from azelic acid loaded nanoemulsion and emulsion. The drug release from azelic acid nanoemulsion and emulsion were presented in Figure 3.10. The present drug release of azelic acid nanoemulsion was observed as 87.78% at 12 hours. The drug release from azelic acid emulsion was comparatively higher than azelic acid nanoemulsion with 98.67 % at 12 hours. The release of azelic acid from azelic acid nanoemulsion was significantly slower compared to azelic acid emulsion (ANOVA, $p < 0.05$). The azelic acid nanoemulsion exhibited controlled burst release phenomenon as well as sustained release characteristics. Obtained data of diffusion-controlled release showed that up to 12.75 ± 0.3 % of azelic acid from nanoemulsion was released over the initial assay stages (the first 1 h) followed by sustained release pattern with low level of burst release and reached 87.67 ± 0.9 % after 12 h.

The drug release is regulated by the interactions of the drug, the surfactants, and the drug partitioning between the aqueous and oil phases. The reduction of drug release from azelic acid nanoemulsion can be correlated to the presence of the gelling agent xanthan gum in nanoemulsion, which induced a complexity of the gel network. Therefore, it is expected to obtain a prolonged release of incorporated azelic acid at the site of application to maintain the supply of the therapeutic agent towards effective skin disorder treatment.

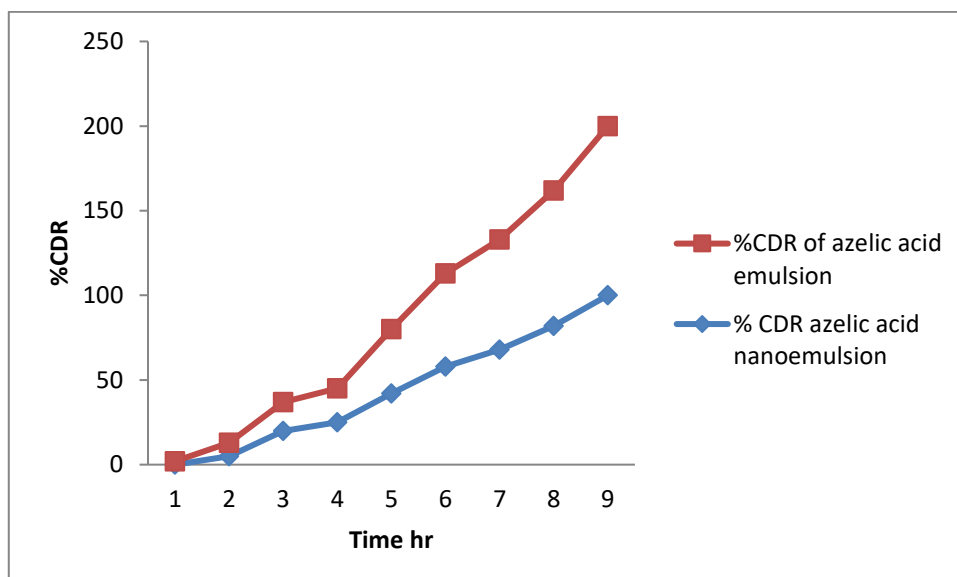
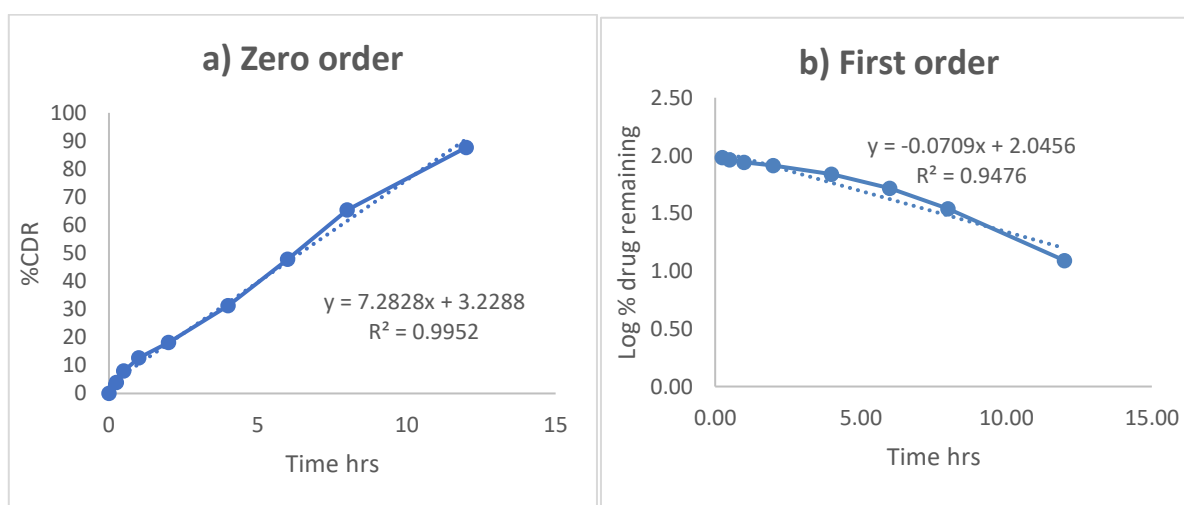


Figure 3.10: Percentage cumulative drug release of azelic acid from a) azelic acid emulsion b) azelic acid nanoemulsion

3.4.13 Kinetic Release Study

To provide a relationship between the results obtained and a possible release mechanism, the data were fitted to various kinetic models such as zero order, first-order, Higuchi, Hixson-Crowell, and Korsmeyer Peppas. The release rate was calculated from the slope of appropriate plots and the regression coefficient (R^2) was determined for all kinetic models for azelic acid release from the nanoemulsion and shown in Figure 3.11. The observed R^2 values for the azelic acid release from azelic acid nanoemulsion were 0.9952 (zero-order model), 0.9932 (Korsmeyer-Peppas), 0.9479 (Higuchi), 0.9487 (first-order) and 0.9795 (Hixson-Crowell).

According to the data shown at the figure 3.11, the profile of azelic acid release from nanoemulsion the best fit to zero order kinetic model. High linearity of the plots was achieved ($R^2 = 0.9941$). It means that the active substance is released slowly, with the constant rate, independent of the initial drug concentration or the amount of drug remaining in the nanoemulsion. A steady amount of the released substances over time can minimize potential side effects because of the reduction in the frequency of drug application and ideal method to achieve a dermatological prolonged action. The similar results, concerning release of drugs from nanosystems were previously reported and showed that the release of nystatin from nanoemulsion-based gel followed zero order kinetic models. In case of the release Azelic acid from the nanoemulsion the release profiles also could be best explained by Korsmeyer-Peppas models due to regression line is characterized by higher R^2 values than initial ($R^2 > 0.98$).



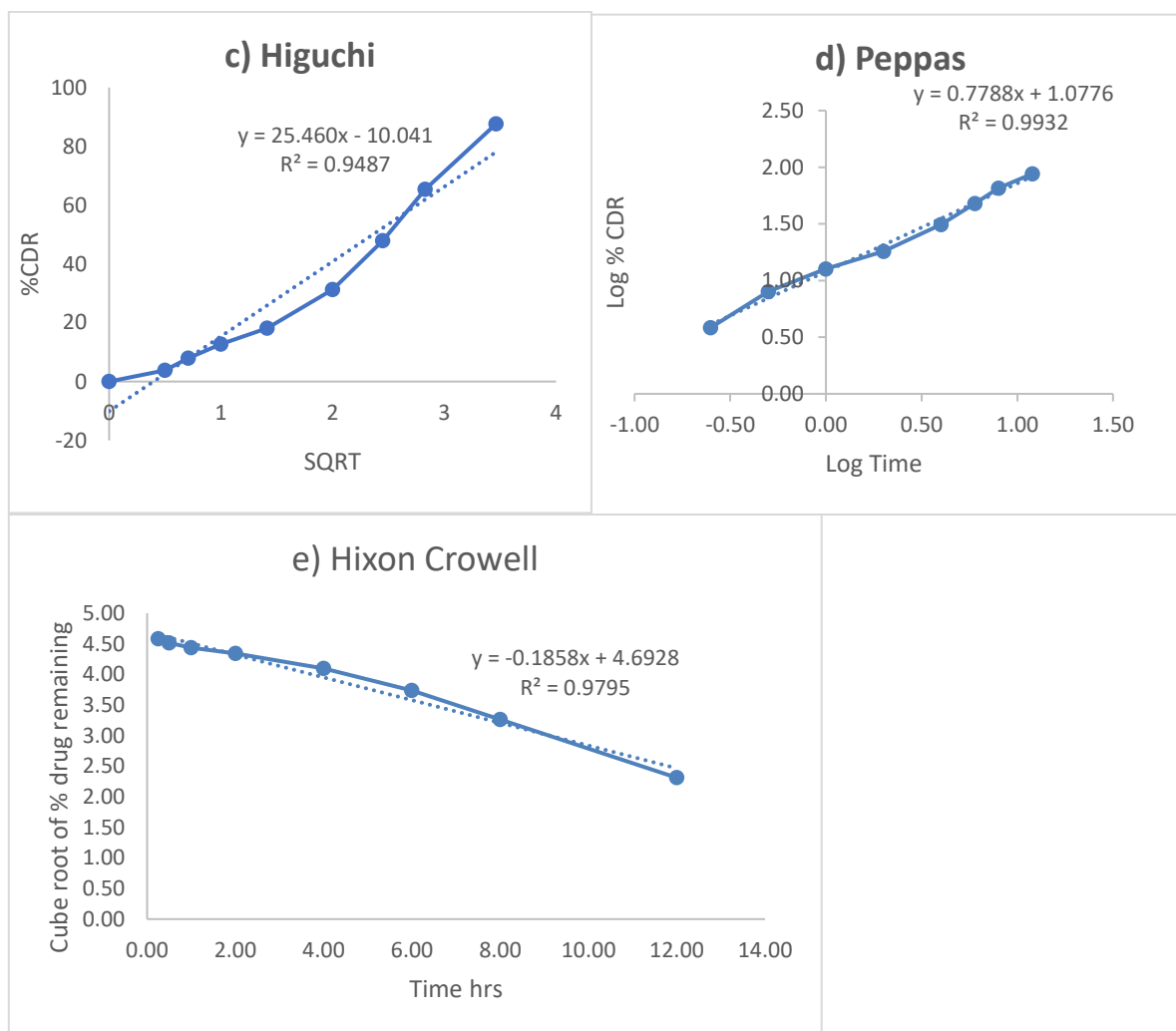


Figure 3.11: Kinetic model of in-vitro release of Azelic acid nanoemulsion a) Zero order b) First order c) Higuchi model d) Peppas Korsmeyer e) Hixon Crowell

3.4.14 Ex-Vivo Permeation studies

Ex vivo permeation experiment (topical delivery) was carried out as a function of time in order to determine the permeation profile of azelic acid nanoemulsion and azelic acid emulsion. In this study, permeation profile of azelic acid -nanoemulsion was compared against azelic acid emulsion in similar concentration across pig skin during 8 h. Figure 3.12 presents plots of ex vivo permeation profiles of azelic acid -nanoemulsion and azelic acid emulsion vs time. The cumulative amount of permeated azelic acid nanoemulsion through skin was obtained $794.29 \mu\text{g}/\text{cm}^2/\text{h}$ after 8 h. The permeation of Azelic acid from Azelic acid -nanoemulsion was obtained 81.20 % and from azelic acid emulsion was obtained 65.23 % through the skin after 8 h. According to the results, from the permeation of Azelic acid form azelic acid nanoemulsion ($81.32 \pm 1.43\%$) across the skin presented significantly ($p < 0.05$) higher compared to the permeation of azelic acid form azelic acid emulsion ($64.88 \pm 1.17\%$).

Some assumptions can be made about the mechanism of the influence of azelic acid nanoemulsion on the penetration of azelic acid in the skin. The high drug loading capacity of nanoemulsion was considered as the first possible mechanism. The permeation enhancers such as surfactant can diffuse on the skin surface because they disrupt the lipid structure of the stratum corneum. This facilitates the diffusion across the barrier that limits the penetration of substances or because of the increase in the solubility of the drug in the skin; that is, it increases the partition coefficient of the drug between the skin and the vehicle. The third possible mechanism depends on the ability of the nanoemulsion droplet to come into intimate contact with the microenvironment of the skin surface due to very small droplet size and very low surface tension.

The fourth possible explanation for enhanced topical delivery may be enhancing effect of the nanoemulsion. Low permeation rate of the drug is expected taking into consideration the hydrophilic nature of azelic acid which has a very low partition coefficient. Incorporation of azelic acid in nanoemulsion formulations significantly increased the transdermal drug flux compared with the emulsion. These results demonstrated

that the formulations developed can modulate the permeation of Azelic acid in the skin, which is precisely the goal of the development of these systems and can allow the azelic acid to stay longer on the skin, where the sites of action are, and not be absorbed. This avoids possible systemic actions of the drug.

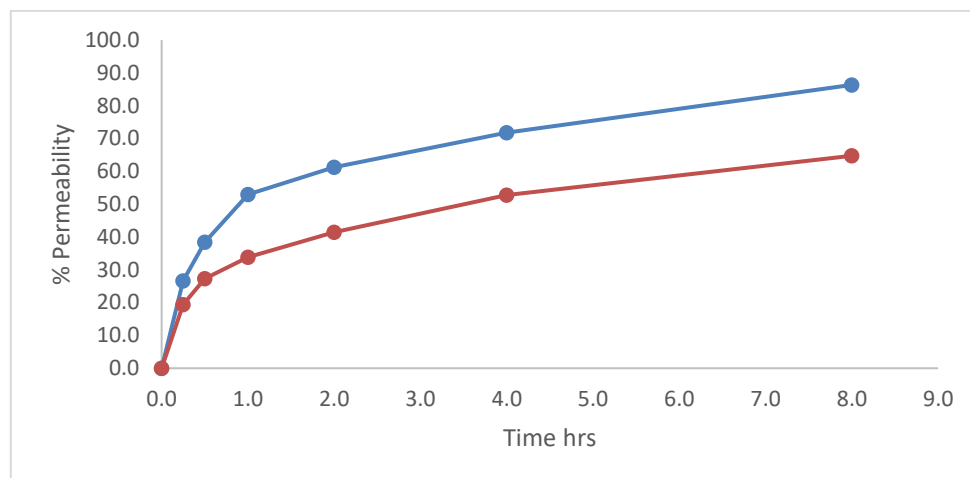


Figure 3.12: Ex-vivo Permeation release of a) azelic acid nanoemulsion b) AZELIC ACID emulsion through pig skin

3.4.15. Skin Retention

The kojic acid-loaded nanoemulsion and emulsion formulations were investigated for azelic acid retention in the deeper layer of the skin. Table 3.15 shows the retention results of azelic acid nanoemulsion and emulsion in skin.

The study showed that azelic acid nanoemulsion ($10.33 \pm 1.23 \mu\text{g}/\text{cm}^2$) showed a significantly increased drug retention value as compared to azelic acid emulsion ($6.011 \pm 1.60 \mu\text{g}/\text{cm}^2$) (ANOVA, $p < 0.01$).

The analysis of the behavior of azelic acid nanoemulsion at the end of 8 hours showed smaller cutaneous retention ($10.55 \mu\text{g}/\text{cm}^2$) possibly because the solution is not lipophilic and does not interact with the lipids present in the skin. Besides that, retention results were reported only for total skin, not occurring separation of SC from viable skin.

Table 3.15: Comparison of retention of azelic acid in the azelic acid nanoemulsion and emulsion for the skin membrane

Sample	Retention in skin membrane [$\mu\text{g}/\text{cm}^2$]
AZELIC ACID nanoemulsion	10.33 ± 1.23
AZELIC ACID emulsion	5.011 ± 1.60

3.5 Conclusion

The azelic acid nanoemulsion was produced by emulsification ultrasonication method and was optimized using Box-Behnken design. Analysis of variance (ANOVA) showed that the fitness of the quadratic polynomial fit the experimental data with significant model F-value, p-value of $p < 0.0500$, and a non-significant lack-of-fit. The optimized formulation of azelic acid nanoemulsion contains globule size, PDI and entrapment efficiency, 185nm, 0.3 and 84.99% respectively. The azelic acid formulation with a Zeta potential value of -35.90 mV demonstrated a higher electrostatic repulsion, which indicated that the nanoemulsion system was stable. SEM and TEM images revealed that experimental formulations displayed small spherical shaped particles with uniformity/homogeneous and uniform azelic acid nanoemulsion formulation.

FTIR, XRD, DSC and TGA results supported the formation of nanoemulsion. In the DSC and FTIR analysis of azelic acid nanoemulsion the peaks of azelic acid indicated that azelic acid was incorporated within the nanoemulsion either in molecularly dispersed state and stabilised in amorphous form and there was no chemical interaction between drug and other ingredients. Thus, the pH of the Azelic acid nanoemulsion was found to be 5.87, in a suitable range for topical applications, indicating its suitability for use as a topical formulation. The shear thinning (pseudo-plastic) formulation exhibited a low viscosity fluid behaviour (low resistance) to flow when tested under high shear conditions. The cosmetic and pharmaceutical industries

usually demand shear thinning behaviour for topical formulation products as they are easy to apply. The percentage release of azelic acid from the azelic acid nanoemulsion and the azelic acid emulsion were 87.66 % and 97.99 % respectively. The release rate of azelic acid from the azelic acid nanoemulsion is slower than azelic acid from the emulsion indicating that nanoemulsion is potential drug-controlled release systems. The value of "R²" of the formulation 0.9952, suggest that the zero-order model is most fitted kinetic model. The solubility, as well as the dissolution, of the azelic acid was enhanced, and this could improve the therapeutic effects of azelic acid.

Stable nanoemulsion of azelic acid was produced as they showed no physical changes or phase separation after being subjected to centrifugation test and freeze-thaw cycle test. A storage stability study was carried out at three different temperatures (5, 25 and 40°C) for 7 weeks, but in the last week of the study observation at 40°C showed slight color change, other than that there was no sign of phase and color changes. pH studies showed that all formulations generally showed a decreasing trend in terms of pH value throughout the period of 7 weeks at different temperatures. Ex-vivo permeation studies of nanoemulsion of azelic acid were performed on pig skin by using Franz diffusion cell. Percent cumulative amount of azelic acid that was permeated from the azelic acid nanoemulsion was more compared to the azelic acid emulsion. The percentage permeability of azelic acid in the skin from azelic acid nanoemulsion was 82.24 % and from azelic acid emulsion was 65.23 %. The azelic acid nanoemulsion produced was stable and has improved action in maintaining skin integrity and complexion.

Permeation studies suggested that the azelic acid nanoemulsion formulation was good in drug retention in the skin and more azelic acid was released in the skin and meanwhile low drug permeability to blood circulation. The Azelic acid nanoemulsion was stable and has improved action. That favoured the use of combination of PVA & Xanthan gum and Transcutol P & tween 80 for topical use. Azelic acid nanoemulsion was more effective as compared to Azelic acid emulsion in the comparative study.

References

1. Sutradhar KB, Amin ML. Nanoemulsions: increasing possibilities in drug delivery. *European Journal of Nanomedicine*. 2013 Jul 1;5(2):97-110.
2. Fernandez P, André V, Rieger J, Kühnle A. Nano-emulsion formation by emulsion phase inversion. *Colloids and Surfaces A: Physicochemical and Engineering Aspects*. 2004 Dec 20;251(1-3):53-8.
3. Gannu R, Palem CR, Yamsani VV, Yamsani SK, Yamsani MR. Enhanced bioavailability of lacidipine via microemulsion based transdermal gels: formulation optimization, ex vivo and in vivo characterization. *International journal of pharmaceutics*. 2010 Mar 30;388(1-2):231-41.
4. Cevc G. Lipid vesicles and other colloids as drug carriers on the skin. *Advanced drug delivery reviews*. 2004 Mar 27;56(5):675-711.
5. Bhasazelic acid r K, Anbu J, Ravichandiran V, Venazelic acid teswarlu V, Rao YM. Lipid nanoparticles for transdermal delivery of flurbiprofen: formulation, in vitro, ex vivo and in vivo studies. *Lipids in health and disease*. 2009 Dec;8(1):1-5.
6. Kong M, Chen XG, Kweon DK, Park HJ. Investigations on skin permeation of hyaluronic acid based nanoemulsion as transdermal carrier. *Carbohydrate Polymers*. 2011 Aug 15;86(2):837-43.
7. Khurana S, Jain NK, Bedi PM. Nanoemulsion based gel for transdermal delivery of meloxicam: physico-chemical, mechanistic investigation. *Life sciences*. 2013 Mar 14;92(6-7):383-92.
8. Ravella V. Nano Emulsion of Azelic acid and Tetrahydro Curcumin Formulation for Hyperpigmentation. *International Journal of Pharmaceutics and Drug Analysis*. 2019;7(6):38-42.
9. Sharma B, Sharma A. Future prospect of nanotechnology in development of anti-ageing formulations. *Int J Pharm Pharm Sci*. 2012;4(3):57-66.
10. Gonçalves ML, Correa MA, Chorilli M. Skin delivery of kojic acid-loaded nanotechnology-based drug delivery systems for the treatment of skin aging. *BioMed Research International*. 2013 Jan 1;2013.
11. Gonçalves ML, Marcussi DG, Calixto GM, Corrêa MA, Chorilli M. Structural characterization and in vitro antioxidant activity of kojic dipalmitate loaded W/O/W multiple emulsions intended for skin disorders. *BioMed research international*. 2015 Jan 1;2015.
12. Jaslina NF, Faujan NH, Mohamad R, Ashari SE. Effect of addition of PVA/PG to oil-in-water nanoemulsion kojic monooleate formulation on droplet size: three-factors response surface optimization and characterization. *Cosmetics*. 2020 Sep 23;7(4):73.
13. Azhar SN, Ashari SE, Ahmad S, Salim N. In vitro kinetic release study, antimicrobial activity and in vivo toxicity profile of a azelic acid ester-based nanoemulsion for topical application. *RSC advances*. 2020;10(71):43894-903.

14. Syed Azhar SN, Ashari SE, Salim N. Development of a kojic monooleate-enriched oil-in-water nanoemulsion as a potential carrier for hyperpigmentation treatment. *International journal of nanomedicine*. 2018 Oct 15;6465-79.
15. Khezri K, Saeedi M, Morteza-Semnani K, Akbari J, Hedayatizadeh-Omran A. A promising and effective platform for delivering hydrophilic depigmenting agents in the treatment of cutaneous hyperpigmentation: Azelic acid nanostructured lipid carrier. *Artificial Cells, Nanomedicine, and Biotechnology*. 2021 Jan 1;49(1):38-47.
16. Al-Edresi S, Baie S. In-vitro and in-vivo evaluation of a photo-protective kojic dipalmitate loaded into nano-creams. *Asian J Pharm Sci*. 2010;5(6):251-65.
17. Costa LC, Louchard BO, Neto EM, da Silva Giffony P, Campos FM, de Araujo TG. Development and Characterization of Azelic acid and Carnaúba Wax-Based Solid Lipid Microparticles. *Journal of Young Pharmacists*. 2020;12(4):309.
18. Lajis AF, Hamid M, Ahmad S, Ariff AB. Lipase-catalyzed synthesis of azelic acid derivative in bioreactors and the analysis of its depigmenting and antioxidant activities. *Cosmetics*. 2017 Jul 4;4(3):22.
19. Kobayashi Y, Azelic acid yahara H, Tadasa K, Naazelic acid mura T, Tanaazelic acid H. Synthesis of amino acid derivatives of azelic acid and their tyrosinase inhibitory activity. *Bioscience, biotechnology, and biochemistry*. 1995 Jan 1;59(9):1745-6.
20. Norddin FA, Azhar SN, Ashari SE. Evaluation of direct esterification of fatty acid derivative of azelic acid in co-solvent system: A statistical approach. *J. Biosens. Bioelectron*. 2017;8:331.
21. Devangamath SS, Lobo B, Masti SP, Narasagoudr S. Thermal, mechanical, and AC electrical studies of PVA-PEG-Ag 2 S polymer hybrid material. *Journal of Materials Science: Materials in Electronics*. 2020 Feb;31:2904-17.
22. Bernal-Chávez SA, Alcalá-Alcalá S, Tapia-Guerrero YS, Magaña JJ, Del Prado-Audelo ML, Leyva-Gómez G. Cross-linked polyvinyl alcohol-xanthan gum hydrogel fabricated by freeze/thaw technique for potential application in soft tissue engineering. *RSC advances*. 2022;12(34):21713-24.
23. Raja PB, Munusamy KR, Perumal V, Ibrahim MN. Characterization of nanomaterial used in nanobioremediation. In *Nano-bioremediation: fundamentals and applications 2022* Jan 1 (pp. 57-83). Elsevier.
24. Kumar R, Singh A, Sharma K, Dhasmana D, Garg N, Siril PF. Preparation, characterization and in vitro cytotoxicity of Fenofibrate and Nabumetone loaded solid lipid nanoparticles. *Materials Science and Engineering: C*. 2020 Jan 1;106:110184.
25. Khezri K, Saeedi M, Morteza-Semnani K, Akbari J, Hedayatizadeh-Omran A. A promising and effective platform for delivering hydrophilic depigmenting agents in the treatment of cutaneous hyperpigmentation: Azelic acid nanostructured lipid carrier. *Artificial Cells, Nanomedicine, and Biotechnology*. 2021 Jan 1;49(1):38-47.
26. Khan BA, Waheed M, Hosny KM, Rizg WY, Murshid SS, Alharbi M, Khan MK. Formulation and Characterization of Carbopol-934 Based Kojic Acid-Loaded Smart Nanocrystals: A Solubility Enhancement Approach. *Polymers*. 2022 Apr 6;14(7):1489.
27. Aziz SB, Abdullah OG, Hussein SA, Ahmed HM. Effect of PVA blending on structural and ion transport properties of CS: AgNt-based polymer electrolyte membrane. *Polymers*. 2017 Nov 15;9(11):622.
28. Kurnool AN, Acharya A, Ramesh B. Approaches to modify the nature of xanthan gum and characterizations to improve its functionality. *Journal of Pharmaceutical Sciences and Research*. 2019;11(1):15-20.
29. Badar R, Yaqoob S, Ahmed A, Shaor QU. Screening and optimization of submerged fermentation of aspergillus species for azelic acid production.
30. Devi KD, Vijayalakshmi P, Shilpa V, Kumar BV. Optimization of cultural parameters for cost effective production of azelic acid by fungal species isolated from soil. *Microbiol. Res. J. Int*. 2015;7(5):255-68.
31. Azelic acid azelic acid zelic acidr R, Singh C. Theoretical study of the azelic acid structure in gas phase and aqueous solution. *International Journal of Quantum Chemistry*. 2011 Dec;111(15):4318-29.
32. Jipa IM, Stoica A, Stroescu M, Dobre LM, Dobre T, Jinga S, Tardei C. Potassium sorbate release from poly (vinyl alcohol)-bacterial cellulose films. *Chemical Papers*. 2012 Feb;66:138-43.
33. Singh CP, Shukla PK, Agrawal SL. Ion transport studies in PVA: NH₄CH₃COO gel polymer electrolytes. *High Performance Polymers*. 2020 Mar;32(2):208-19.
34. Reis EF, Campos FS, Lage AP, Leite RC, Heneine LG, Vasconcelos WL, Lobato ZI, Mansur HS. Synthesis and characterization of poly (vinyl alcohol) hydrogels and hybrids for rMPB70 protein adsorption. *Materials Research*. 2006;9:185-91.

35. Kharazmi A, Faraji N, Hussin RM, Saion E, Yunus WM, Behzad K. Structural, optical, opto-thermal and thermal properties of ZnS–PVA nanofluids synthesized through a radiolytic approach. *Beilstein journal of nanotechnology*. 2015 Feb 23;6(1):529-36.
36. Choo K, Ching YC, Chuah CH, Julai S, Liou NS. Preparation and characterization of polyvinyl alcohol-chitosan composite films reinforced with cellulose nanofiber. *Materials*. 2016 Jul 29;9(8):644.
37. Faria S, de Oliveira Petkowicz CL, De Moraes SA, Terrones MG, De Resende MM, de Franca FP, Cardoso VL. Characterization of xanthan gum produced from sugar cane broth. *Carbohydrate polymers*. 2011 Aug 15;86(2):469-76.
38. Osiro D, Franco RW, Colnago LA. Spectroscopic characterization of the exopolysaccharide of *Xanthomonas axonopodispv. citri* in Cu²⁺ resistance mechanism. *Journal of the Brazilian Chemical Society*. 2011;22:1339-45.
39. Ruby JJ, Pandey VP. Selection of excipients for memantine hydrochloride nanoparticles through drug excipient compatibility testing. *Int. J. Pharm. Tech Res.*. 2015;7:22-6.
40. Aziz SB. Modifying poly (vinyl alcohol)(PVA) from insulator to small-bandgap polymer: A novel approach for organic solar cells and optoelectronic devices. *Journal of Electronic Materials*. 2016 Jan;45(1):736-45.
41. Kumbhar SA, Koazelic acid re CR, Shrivastava B, Choudhury H. Specific and Sensitive RP-HPLC Method Development and Validation for the Determination of Aripiprazole: Application in Preformulation Screening of Nanoemulsion. *Current Nanomedicine (Formerly: Recent Patents on Nanomedicine)*. 2020 Mar 1;10(1):76-86.
42. Modi JD, Patel JK. Nanoemulsion-based gel formulation of aceclofenac for topical delivery. *International Journal of Pharmacy and Pharmaceutical Science Research*. 2011;1(1):6-12.
43. Khajeh M, Zadeh FM. Response surface modeling of ultrasound-assisted dispersive liquid–liquid microextraction for determination of benzene, toluene and xylenes in water samples: Box–Behnken design. *Bulletin of environmental contamination and toxicology*. 2012 Jul;89:38-43.
44. Shakeel F, Haq N, Alanazi FK, Alsarra IA. Box-Behnken statistical design for removal of methylene blue from its aqueous solution using SDS self-microemulsifying systems. *Ind. Eng. Chem. Res.* 2014;53:1179-88.
45. Amenaghawon NA, Nwaru KI, Aisien FA, Ogbeide SE, Okieimen CO. Application of Box-Behnken design for the optimization of citric acid production from corn starch using *Aspergillus niger*. *British Biotechnology Journal*. 2013 Jul 1;3(3):236.